Journal of Ceramic Processing Research. Vol. 13, Special. 1, pp. s70~s74 (2012)

J O U R N A L O F
Ceramic Processing Research

Effect of multi-buffer layer on the quality of ZnO thin films deposited on quartz substrate by magnetron sputtering

Du-han Bae and Geun-Hyoung Lee*

Department of Materials & Components Engineering, Electro Ceramic Center, Dong-eui University, 995 Eomgwangno, Busanjigu, Busan, 614-714, Korea

ZnO thin films were prepared with ZnO multi-buffer layers by a magnetron sputtering system. ZnO thin films with mono-buffer layer and without buffer layer were also prepared. The films were characterized with X-ray diffraction (XRD), field emission scanning electron microscopy (FE-SEM), dynamic force microscope (DFM) and ultraviolet-visible spectroscopy (UV-Vis). The ZnO films with buffer layers showed the improvement in crystalline quality and the release of lattice strain, while the film without buffer layer showed the shift of peak position in XRD spectra. The improvement in the surface smoothness of the film with multi-buffer layer was observed by FE-SEM and DFM. UV-Vis analysis showed that all samples exhibited more than 70% transmittance in the visible region. The steepest fall-off near band edge was found in the transmittance spectrum of the film with multi-buffer layer.

Key word : ZnO, Buffer layer, Magnetron sputtering.

Introduction

The semiconductor ZnO has been attracted a great attention due to its excellent properties such as its wide direct band gap of 3.37 eV and large exciton binding energy of 60 meV, which makes ZnO possible for potential applications in efficient room-temperature exciton-based emitters and low threshold semiconductor lasers [1]. Because of these properties, ZnO is considered as a promising material for a variety of applications by realizing P-N junctions, including room-temperature ultraviolet laser [2], sensors [3], photocatalysts [4], solar cells [5] and field-emission devices [6].

ZnO films have been fabricated by various methods such as sputtering [7], sol-gel process [8], spray pyrolysis [9], pulsed laser deposition [10], atomic layer deposition [11], molecular beam deposition [12] and chemical vapor deposition [13]. Among them, sputtering is one of the convenient deposition techniques to deposit films uniformly on the large area. In this work, sputtering method was employed to deposit the ZnO films.

The improvement of thin film quality on the crystal structure and surface morphology can directly affect on the performance of applied devices. Therefore, various efforts have been made in order to improve the quality of thin film. In the current applications, a mono-buffer layer prior to the deposition of main thin film has been widely employed due to its simple and effective process. Previous works confirmed that the buffer layer was very effective for the improvement of the quality of ZnO thin film because the buffer layer released the stress resulted from lattice mismatch between thin film and substrate [14-16]. ZnO thin film with homo buffer layer has been also extensively studied with various methods [17-19]. Many reports have studied the effect of ZnO mono-buffer layer on the crystalline quality of ZnO film, but few have reported on the effect of ZnO multi-buffer layer on ZnO crystalline quality.

In this paper, the effect of multi-buffer layer on the crystalline quality and surface morphology of ZnO film is investigated. The each layer in multi-buffer layer was deposited at different temperatures, leading to the improvement in the crystalline quality and surface morphology of ZnO film.

Experimental details

ZnO thin films were grown on quartz substrates by a magnetron sputtering system. Three series of samples were prepared. The first one was the ZnO thin film with a thickness of 260 nm deposited at 600 °C without buffer layer (sample 1). The second series consisted of samples with mono-buffer layer. Three samples with mono-buffer layer were prepared. ZnO mono-buffer layers were deposited on the substrates prior to the deposition of ZnO main films. The thicknesses of mono-buffer layers were set at 60 nm. For each sample, mono-buffer layers were deposited at different temperatures of 300 °C (sample 2), 400 °C (sample 3) and 500 °C (sample 4). The third one was the sample grown on multi-buffer layer (sample 5), which was composed of three layers. Each layer of multi-buffer layer was

*Corresponding author:
Tel : +82-51-890-1722
Fax: +82-51-890-2631
E-mail: ghl@deu.ac.kr

deposited at different temperatures of 300 °C, 400 °C and 500 °C with a thickness of 20 nm. ZnO main films were deposited on the buffer layers with a thickness of 200 nm at 600 °C for samples (2-5). Thus the samples (2-5) had a total thickness of 260 nm. A pure ZnO target (99.99%) was used as a target. Prior to the deposition, quart substrate was loaded into the sputtering chamber and then the chamber was evacuated to 5×10^{-6} torr. The substrate was rotated at 3 rpm for the uniform growth. High-purity Ar and O_2 gases (volume ratio of $Ar:O_2 = 10:1$) were introduced into the chamber during the deposition. The deposition was performed at working pressure of 1.8 mtorr and r.f. power of 150 W.

X-ray diffraction (PANalytical, X'Pert PRO MPD, Netherlands) was employed to characterize the crystal structure of thin films with Cu Kα radiation (λ = 1.5406 Å). The X-ray source was operated at a power of 40 kV×30 mA. Surface morphologies of the samples were investigated by FE-SEM (Quanta 200 FEG, FEI Company) at a voltage of 30 kV and DFM (L-trace II, SII Nano Technology). Transmittance spectra were obtained by UV-Vis (S-3100, Scinco) with the average scan number of 30 on air base in the wavelength range of 200~800 nm.

Results and discussion

Fig. 1(a) shows the X-ray diffraction patterns of the samples. For all samples, only (002) and (004) diffraction peaks of ZnO phase were detected, indicating that all the ZnO films were well grown along the c-axis orientation. As shown in Fig. 1(a), the intensity of (002) peak in the XRD spectrum of sample 5 was strongest, which means that the ZnO film grown on multi-buffer layer has the best crystalline quality. Fig. 1(b) exhibits the magnified (002) peaks of the samples. The diffraction angles of the (002) peaks were 34.64°, 34.40°, 34.45°, 34.44° and 34.42° for sample 1 to 5, respectively. The (002) peak position of the sample 5 (ZnO film with multi-buffer layer) is very close to the bulk value of 34.43°, indicating their high crystalline quality. The shift in the (002) peak position toward the higher angle for the sample 1 is observed. This can be attributed to the stress from the lattice mismatch between substrate and thin film. The c-axis lattice parameters are calculated by using Bragg's law.

The calculated c-axis lattice parameters are shown in Table 1. The values are 5.175, 5.209, 5.202, 5.204 and 5.207 Å for sample 1 to 5, respectively. The c-axis lattice parameter of 5.207 Å which is close to the bulk value of 5.207 Å was observed for the film grown on multi-buffer layer (sample 5), while the c-axis lattice parameter of 5.172 Å was observed for the film without buffer layer (sample 1). This implies that many vacancy defects exist in sample 1 with stress along the c-axis. However, compared to the film without buffer layer (sample 1), the films grown on buffer layers (sample 2-5) also show the improvement in the crystalline quality and the relaxation of the lattice mismatch.

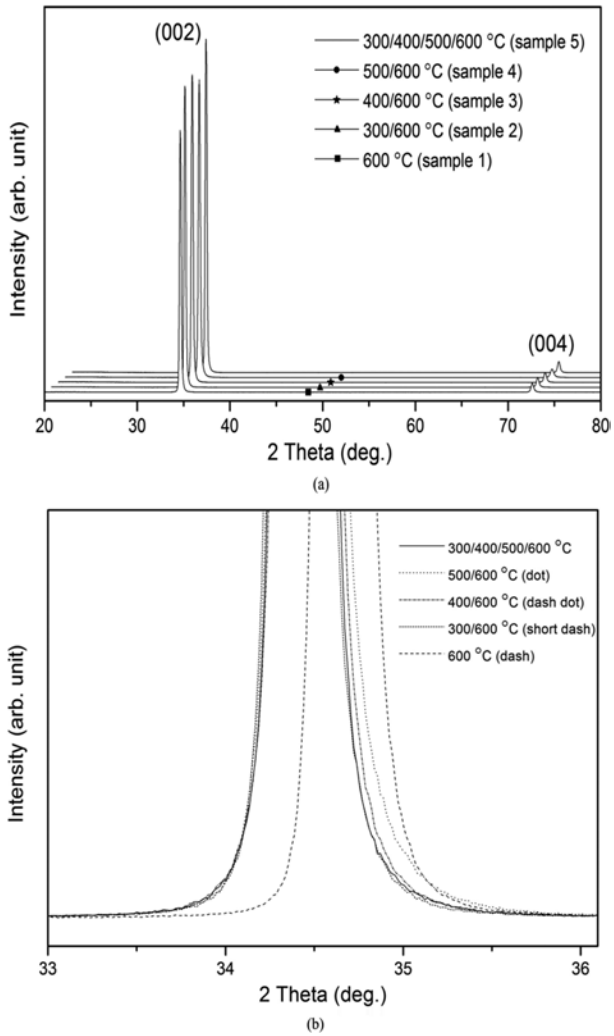

Fig. 1. XRD patterns of samples. The (002) facet patterns are magnified in (b) and the shift of sample 1 can be seen.

Table 1. Summary of c-axis lattice parameter for the samples.

	Smaple 1	Sample 2	Sample 3	Sample 4	Sample 5	Bulk
c-axis lattice parameter	5.175 Å	5.209 Å	5.202 Å	5.204 Å	5.207 Å	5.207 Å

The c-axis lattice parameter was calculated from Bragg's Law (λ = 1.5406Å).

The SEM images of the samples are shown in Fig 2. The flat and mirror-like surface is observed for sample 2 and sample 5. However, the rough surface which is composed of grains with large size and irregular shape is observed on the surface of other samples. This result respects that the two dimensional growth is preferred rather than three dimensional growth for sample 2 and sample 5. DFM images were also employed to investigate the surface morphologies in more details. The DFM

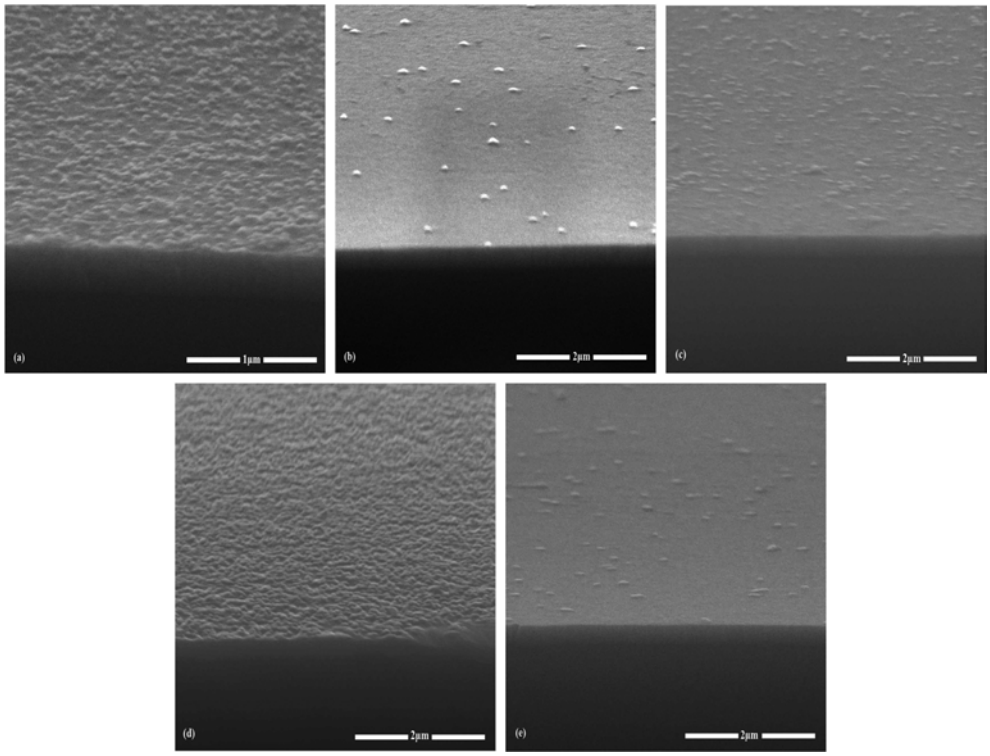

Fig. 2. SEM images of each sample. The improvement of surface morphology is observed in Fig. 2 (b) and (e).

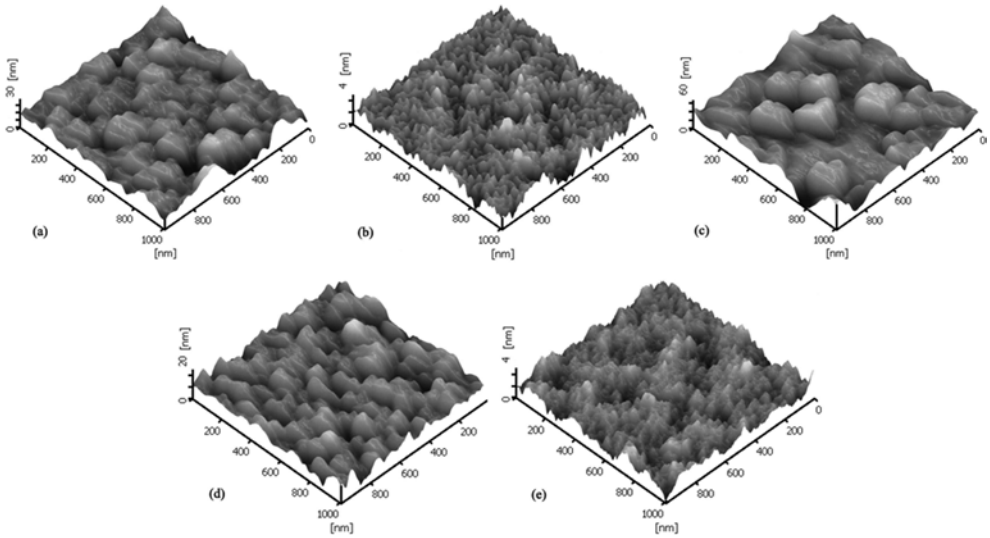

Fig. 3. DFM images of each sample. Root mean square (RMS) values of each sample refer to (a) 4.523 nm, (b) 0.5946 nm, (c) 9.983 nm, (d) 3.391 nm and (e) 0.6062 nm.

images of the samples are shown in Fig 3. The surface roughness was estimated as root mean square (RMS) values of a surface profile. The RMS values were 4.523 nm, 0.5946 nm, 9.983 nm, 3.391 nm and 0.6062 nm for sample 1 to 5, respectively. These results correspond to the results of SEM. In addition, the large grain size and high RMS values were also observed for the thin films with mono buffer layer (sample 3-4). It is ascribed to the growth temperature of buffer layer. The grain size increases as the growth temperature increases due to the enhancement of the atomic migration ability. Accordingly, with increasing the growth temperature of buffer layer from 300 °C (sample 2 and 5) to 400 °C (sample 3) and 500 °C (sample 4), the film consisted of large grains and its surface became rough.

Fig. 4 (a) shows transmittance spectra of the samples. High transmittance over 70% in the visual region was observed for all samples. The steepest fall-off near band edge is observed in the transmittance spectrum of the sample 5. The optical band gaps of the samples were calculated from the transmittance data. Transmittance was firstly converted to absorbance and then the absorption

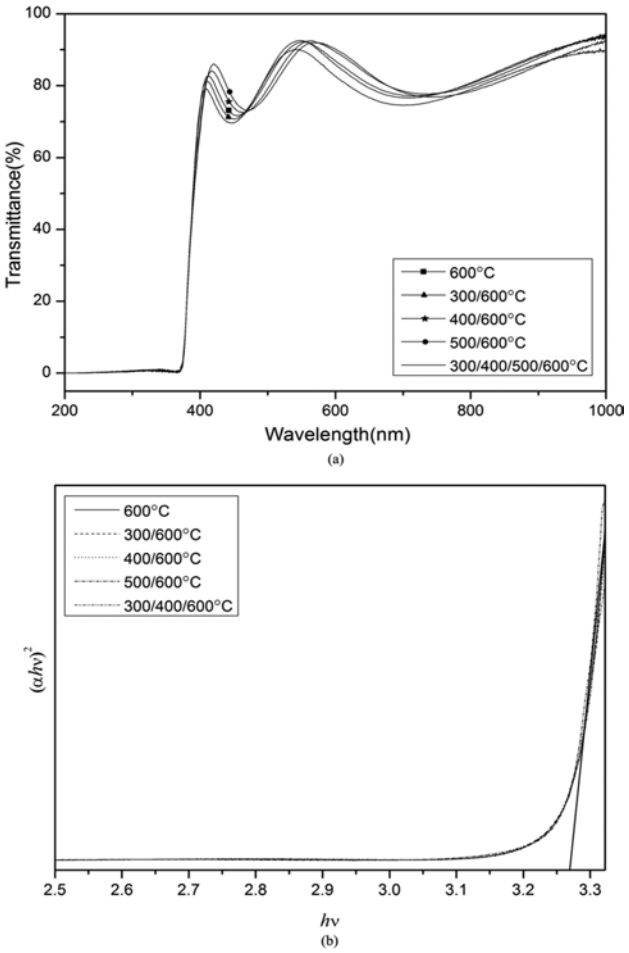

Fig. 4. Transmittance spectra of samples are shown in (a) and plotted $(\alpha h\nu)^2$ vs $h\nu$ spectra, in which α is the absorption coefficient and $h\nu$ is the photon energy, are shown in (b). The optical band gaps were estimated to be 3.27 eV for all the samples by extrapolating the straight line portion of this plot to the energy axis.

coefficient was calculated as a function of photon energy from absorbance versus wavelength curve. The band gaps were obtained by plotting $(\alpha h\nu)^2$ vs $h\nu$, in which α is the absorption coefficient and $h\nu$ is the photon energy, and extrapolating the straight line portion of this plot to the energy axis. The optical band gaps were estimated to be 3.27 eV for all the samples as shown in Fig. 4(b).

These results can conclude that the introduction of low temperature (LT) buffer layer is very effective for the improvement in the crystalline quality and the surface smoothness of ZnO film. In particular, as the deposition temperature of buffer layer decreased, the crystalline quality and the surface smoothness of ZnO film were significantly improved. It is well known that the LT buffer layer provides the nucleation sites and in-plane information of crystals so that the following growth at high temperature can be relaxed and recrystallized [17]. Other research group reported that ZnO buffer layer can be grown easily on the substrate at low temperature due to the large sticking coefficient and amorphous growth mode [20]. The amorphous ZnO buffer layer confines most of dislocations generated at the interface between the substrate and the ZnO thin film, leading to the growth of ZnO main film with high crystalline quality. On the other hand, the crystalline quality of the ZnO film grown on multi-buffer layer was superior to the ZnO films with mono-buffer layer. The multi-buffer layer can be considered to be a thin film with double buffer layers. The first buffer layer grown at a temperature as low as 300 °C acts as a LT buffer layer. The second buffer layer grown on the first LT buffer layer has relatively high crystalline quality because the first LT buffer layer accommodates the lattice stress. The third buffer layer must have higher crystalline quality because it grows on the second buffer layer with high crystalline quality. Therefore, the defects originated from the lattice mismatch between substrate and ZnO thin film can be gradually reduced during the growth of multi-buffer layer. As a consequence, the multi-buffer layer provides a high quality buffer layer at the interface for the following growth of ZnO main film. In the surface morphology, the thin film grown on high temperature (HT) mono-buffer layer (over 400 °C) showed rough surface in the results of both SEM and DFM. In addition, the thin film grown on LT buffer layer occasionally showed rough surface in the previous report [21] while crystalline quality was improved. However, the multi-buffer layer can improve the surface smoothness even though HT buffer layers were employed to introduce the multi-buffer layer. As the growth temperature of buffer layer increases gradually, the mean free path of adatoms on the growing surface gets longer. This enhances the lateral growth of thin film, resulting in the enhancement of two dimensional growth mode. Consequently, the surface of film becomes smooth. These suggest that the employment of multi-buffer layer is more beneficial than mono-buffer layer for the fabrication of ZnO film with high crystalline quality and smooth surface.

Conclusions

The effect of multi-buffer layer on the crystalline quality and surface smoothness of ZnO film was investigated. ZnO films with mono-buffer layer and without buffer layer were also prepared for the comparison. Compared to the ZnO film deposited without buffer layer, ZnO films with higher crystalline quality and smoother surface were fabricated by using buffer layer. As the deposition temperature of buffer layer decreased, the crystalline quality and surface smoothness of ZnO film became better. The ZnO film with the highest crystalline quality and the smoothest surface was achieved by employing multi-buffer layer, in which each buffer layer was deposited at progressively higher temperature. The result indicates that the multi-buffer layer is very effective to improve both the crystalline quality and the surface smoothness of ZnO film.

References

1. Ü. Özgür, Ya. I. Alivov, C. Liu, A. Teke, M.A. Reshchikov, S. Doğan, V. Avrutin, S.J. Cho, H.Morkoç, J. Appl. Phys. 98 (2005) 41301.
2. H. Cao, J.Y. Xu, D.Z. Zhang, S.H. Chang, S.T. Ho, E.W. Seelig, X. Liu, R.P.H. Chang, Phys. Rev. Lett. 84 (2000) 5584.
3. T. Shibata, K. Unno, E. Makino, Y. Ito, S. Shimada, Sens. Actuators A 102 (2002) 106.
4. H. Yumoto, T. Inoue, S.J. Li, T. Sako, K. Nishiyama, Thin Solid Films 345 (1999) 38.
5. K. Keis, L. Vayssieres, S.E. Lindquist, A. Hagfeldt, Nanostruct. Mater. 12 (1999) 487.
6. Y.W. Zhu, H.Z. Zhang, X.C. Sun, S.Q. Feng, J. Xu, Q. Zhao, B. Xiang, R.M. Wang, D.P. Yu, Appl. Phys. Lett. 83 (2003) 144.
7. S. Maniv, A. Zangvil, J. Appl. Phys. 49 (5) (May 1978) 2787.
8. J.H. Lee, K.H. Ko, B.O. Park, J. Cryst. Growth 247 (2003) 119.
9. R. Ayouchi, F. Martin, D. Leinen, J.R. Ramos-Barrado, J. Cryst. Growth 247 (2003) 497.
10. H. Kim, J.S. Horwitz, S.B. Qadri, D.B. Chrisey, Thin Solid Films 420 (2002) 107.
11. A. Yamada, B. Sang, M. Konagai, Appl. Surf. Sci. 112 (1997) 216.
12. K. Nakamura, T. Shoji, K. Hee-Bog, Jpn. J. Appl. Phys., Part 2: Letters 39 (6) (2000) L534.
13. T. Minami, H. Sonohara, S. Takata, H. Sato, Jpn. J. Appl. Phys., Part 2: Letters 33 (5B) (May 15, 1994) L743.
14. A. Setiawan, H.J. Ko, S.K. Hong, Y. Chen, T. Yao, Thin Solid Films 445 (2003) 213.
15. J. Zhu, B. Lin, X. Sun, R. Yao, C. Shi, Z. Fu, Thin Solid Films 478 (2005) 218.
16. L. Xu, L. Shi, X. Li, Appl. Surf. Sci. 255 (2008) 3230.
17. S.H. Jeong, I.S. Kim, J.K. Kim, B.T. Lee, J. Cryst. Growth 264 (2004) 327.
18. Y. Zhang, G. Du, B. Liu, H. Zhu, T. Yang, W. Li, D. Liu, S. Yang, J. Cryst. Growth 262 (2004) 456.
19. K.H. Bang, D.K. Hwang, J.M. Myoung, Appl. Surf. Sci. 207 (2003) 359.
20. J.F. Yan, Y.M. Lu, Y.C. Liu, H.W. Liang, B.H. Li, D.Z. Shen, J.Y. Zhang, X.W. Fan, J. Cryst. Growth 266 (2004) 505.
21. V. Khranovskyy, R. Minikayev, S. Trushkin, G. Lashkarev, V. Lazorenko, U. Grossner, W. Paszkowicz, A. Suchocki, B. G. Svensson, R. Yakimova, J. Cryst. Growth 308 (2007) 93.